

Discrete Tone Emission from High-Pressure Ratio Supersonic Jets from Convergent-Divergent Nozzles

Adnan M. Abdel-Fattah*

Defence Science and Technology Organization, Melbourne, Australia

The results of a test program to investigate the discrete tone generation from free axisymmetric supersonic jets issuing from convergent-divergent conical nozzles of different sizes and expansion ratios in a range of stagnation pressure ratio never reported before are presented. In both highly overexpanded and underexpanded jet conditions, the second shock-cell length was found to be in good agreement with Pack's modified theoretical formula for the first shock-cell length of slightly incorrectly expanded supersonic jets, when the nozzle diameter was replaced by the jet diameter d_j corresponding to the fully expanded jet Mach number M_j . The use of d_j in normalizing shock-associated noise data was first proposed by Tam and Tanna. To a good approximation, the second shock-cell length displayed a linear dependence on the parameter $\beta^2 = M_j^2 - 1$ rather than on β . The apparent length of the first shock cell was also found to display linear dependence on β^2 but only in the overexpanded jet condition. The linear variation of the second shock-cell length with β^2 was found to be invariant for all the nozzles tested, but in the case of the first shock cell, the proportionality constant varied with the nozzle expansion ratio. The discrete tone fundamental frequency was found not to depend on the nozzle exit diameter but to be inversely proportional to the nozzle throat diameter. With a constant ratio between the disturbance convection velocity and the fully expanded jet velocity, the combination of Powell's simplified feedback loop equation with the shock-cell length obtained from the modified theoretical formula predicted to a good practical accuracy the discrete tone fundamental frequency.

Nomenclature

A	= nozzle cross-sectional area
c_o	= ambient speed of sound
d	= nozzle diameter, jet diameter
f	= frequency of the fundamental discrete tone
k	= proportionality constant
L	= shock cell length
\bar{L}	= average shock cell length, cell length near the screech source
M_j	= fully expanded jet Mach number corresponding to the isentropic expansion of the jet from P_o to P_a
P_e	= static pressure at the nozzle exit
P_o	= jet stagnation pressure
P_a	= ambient static pressure
S	= nozzle flow separation at the exit
u_c	= disturbance convection velocity
V_j	= fully expanded jet velocity
β^2	= $(M_j^2 - 1)$
λ	= wavelength of the fundamental discrete tone
γ	= ratio of specific heats

Subscripts

e	= nozzle exit
$*$	= nozzle throat
j	= fully expanded jet condition
1, 2, 3, etc.	= 1st, 2nd, 3rd, etc., shock cells

Introduction

It is well known that gas jets tend to emit acoustic tones at discrete frequencies that are a function of characteristic linear dimensions of nozzle or jet geometry. The phenomena

that cause such emissions are important to the jet-mixing behavior. In the case of confined jets such as may occur in thrust-augmenting ejectors or ramrocket secondary combustion chambers, coupling of the jet frequencies with the natural frequencies of the confining duct can have a profound effect on the mixing and entrainment characteristics.¹⁻³

As part of an investigation of duct resonance and its effect on jet mixing, discrete tone emission from unconfined supersonic freejets and its relationship to shock-cell dimensions has been studied experimentally with a range of axisymmetric convergent-divergent conical nozzles in a range of jet stagnation pressures up to 60 atm. This study was carried out to provide basic data relevant to the resonance behavior of confining ducts when matched to the same nozzles. To the best knowledge of the author, the current experiments extended to a range of jet stagnation pressures that have not previously been covered in published literature on the subject of acoustic emission from jets.

Background

Discrete tones of acoustic radiation, often called screech, are emitted from incorrectly expanded supersonic jets. In his pioneer work, Powell^{4,5} was the first to recognize and study the nature of this type of discrete tones. Qualitatively, he postulated a feedback mechanism or a resonant self-maintained loop for their generation. He deduced a simple loop equation relating to the mechanism's three main components, which are the shock-cell length, disturbance spacing, and the discrete tone wavelength. In its approximate simplified form, which has nevertheless proven to be very useful,^{4-6,11} the loop equation is as follows:

$$\lambda/L = 1 + c_o/u_c \quad (1)$$

Since Powell's pioneer work, the results of many experimental investigations have appeared in the literature. Experimenting with choked axisymmetric jets with P_o/P_a up to 4.5, Davies and Oldfield⁶ confirmed and extended Powell's results. The feedback mechanism was at least qualitatively confirmed by Hammitt,⁷ Glass,⁸ Jungowski,⁹ and, more recently, by

Received Dec. 15, 1986; revision received Jan. 5, 1987. Copyright © American Institute of Aeronautics and Astronautics, Inc., 1987. All rights reserved.

*Senior Research Scientist, Aero Propulsion Division, Aeronautical Research Laboratories.

Nagel et al.¹⁰ in that the use of sound absorbing materials placed on the nozzle lip and other reflecting surfaces were able to interrupt the loop and reduce or eliminate screech. Quantitative verification of Powell's model was presented by Norum¹¹ through detailed directivity measurements. With the aid of high-speed motion photography, Lassiter and Hubbard,¹² and later Sharman et al.,¹³ were able to show the shock-cell structure to be unstable during screech and the shocks to oscillate at the frequency of the fundamental screech tone. Studying the nearfield of the jet, the feedback mechanism was reexamined and confirmed by Yu and Seiner,¹⁴ and in a recent paper by Tam et al.¹⁵ they showed screech tones to be special cases of broadband shock-associated noise, and they provided theoretical and semiempirical formulas for their prediction.

Most of the discrete tone measurements reported by previous researchers were for choked sonic nozzles in a range of jet P_o/P_a up to 6 atm, which is very low compared with those of the current investigation. In a higher pressure range up to 20 atm, Mamin et al.¹⁶ investigated the screech tone phenomenon with axisymmetric jets issuing from convergent-divergent nozzles. They found the discrete tone frequency to be inversely proportional to the nozzle throat diameter, and they presented empirical relations for the discrete tone frequency and for shock-cell lengths.

An important aspect of the study of shock-associated noise, both discrete tone and broadband, is the accurate evaluation of the shock-cell length in the cellular jet plume. The first theoretical prediction for the first shock cell length of a slightly incorrectly expanded axisymmetric supersonic jet was formulated by Prandtl (cited in Ref. 17), who found it to vary as $L_1/de = k\beta$, where $k = 1.306$. Almost half a century later, Pack¹⁷ studied the same problem theoretically but with different boundary conditions. He contended that the proportionality constant k in Prandtl's formula should be in the range 1.2–1.24 instead of 1.306, and he obtained good agreement with the available experimental data at that time. Since then, a considerable amount of data for jets issuing from convergent nozzles in a relatively low range of jet P_o/P_a has appeared in the literature.^{4,6,18} This shows that for the first shock cell, k varies in the range 1.3–1.5. For the second shock cell, Harper-Bourne and Fisher¹⁸ found L_2 to vary linearly with β as predicted by Pack in the range up to $P_o/P_a = 4$ before it started to deviate from this linear dependence on β . Experimenting with conical convergent-divergent nozzles in a very high-pressure range up to $P_o/P_a = 200$, Love et al.¹⁹ presented semiempirical formulas for L_1 prediction. Seiner and Norum²⁰ noticed differences between the shock-cell spacings of jets issuing from incorrectly expanded convergent and convergent-divergent nozzles. In both cases, L_2 varied linearly with β as predicted by Pack, but that of the Mach 2 nozzle appeared to grow faster by a factor equal to V_e/V_* . Recently, more theoretical predictions for the shock-cell length have appeared in the literature. In the vortex-sheet shock-cell model solution used by Tam and Tanna,²¹ they were the first to propose the use of a hypothetical shock-cell length L_j that corresponds to the fully expanded jet diameter d_j . With this, they obtained good agreement with their measured broadband shock-noise peak frequency. Better agreement was achieved with a model developed by Tam et al.²² through the use of multiple scales method.

In Powell's feedback mechanism, the relevant shock-cell length is that in the vicinity of the effective screech source in the shear layer downstream of the nozzle exit. It is generally agreed that, as has been found experimentally by several investigators, the effective source is located at or downstream of the end of the third shock cell.^{4,5,7,8,13,14,26} The shock-cell length decreases with distance downstream of the nozzle due to viscous and mixing effects, and its accurate measurement at downstream locations is sometimes very difficult. This is because that at these locations the jet is often unstable; the shock cells are obscured by turbulence in the jet, and the

shocks in the shear layer are too dispersed to form a clear image, especially at their extremities where measurements are performed. Usually an average value \bar{L} is used in Eq. (1) and this is obtained by dividing the length of the potential core of the jet by the number of shock cells. Powell⁵ suggested \bar{L} to be 80% of L_1 ; Harper-Bourne and Fisher¹⁸ found it to be 88% of L_2 ; Norum¹¹ used a value of 90% of L_3 , and Tam et al.¹⁵ used a value of 80% of L_j .

The value for the disturbance convection velocity u_c is well-established experimentally and readily available in the literature; therefore, no attempt was made to measure its value in the current investigation. It is generally accepted that a nominal value of $u_c/V_j = 0.70 \pm 0.05$ to be of reasonable accuracy.^{4,11,15,18,21,24–27} Other values reported for u_c/V_j are 0.70–0.80 by Lowson and Ollerhead²⁵ and 0.815 by Mamin et al.¹⁶

Experimental Apparatus

Tests were conducted with two families of convergent-divergent conical nozzles of fixed half-angle of 7.13 deg; particulars are shown in Table 1. The first family consisted of five geometrically similar but differently sized nozzles, with a fixed expansion ratio $A_e/A^* = 4.04$. The other family consisted of four nozzles of fixed throat diameter $d^* = 9.2$ mm but with varying expansion ratio.

Unheated air was supplied from storage vessels over a regulated pressure range of up to 60 atm. The noise generated was measured with a Bruel & Kjaer 13.2 mm condenser microphone located at a fixed position 50 deg upstream from the nozzle exit in a horizontal plane containing the nozzle centerline at radius of 148 mm. The microphone signal was connected to a sound-level meter and to a four-channel tape recorder. The recorded signal was analyzed and the spectrum plotted with a Spectral Dynamics Corporation model SD335 spectroscopy real-time analyzer. The jet flowfield was observed with a conventional schlieren system with high-intensity spark of about 0.5 μ s duration, which was short enough to freeze the high-speed jet flowfield and associated emitted phenomena. The shock-cell spacings were directly measured from the schlieren photographs.

Results and Discussion

Since current investigation covered both the highly underexpanded and overexpanded ranges of jet-pressure ratio for each nozzle, tests were carried out to determine the conditions for which nozzle separation occurs as a prelude to the discussion of the results. This was performed by measuring the nozzle static pressure P_e with a static pressure tapping very close to the nozzle exit. Figure 1 shows the results obtained with nozzle D and nozzle 1 of the first and second families respectively in terms of P_e/P_a vs P_o/P_a . Shown also in Fig. 1 for both nozzles the theoretical variation P_e/P_a vs P_o/P_a obtained from the relation $P_e/P_a = (P_o/P_a)/(P_o/P_a)_D$, where the subscript D refers to the design nozzle exit condition corresponding to A_e/A^* for each nozzle at which $P_e/P_a = 1$.

Table 1 Particulars of the convergent-divergent nozzles used in the current experiments

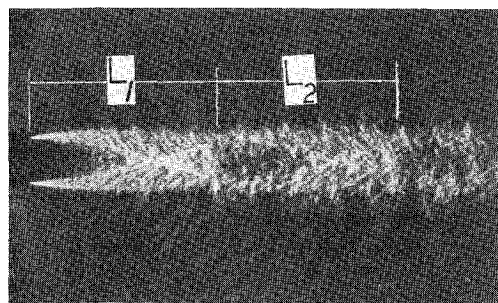
Nozzle	d_* , mm	D_e , mm	A_e/A^*	M (exit)
A	5.56	11.19	4.04	2.95
B	6.18	12.42	4.04	2.95
C	7.75	15.56	4.04	2.95
D	9.25	18.55	4.04	2.95
E	12.32	24.74	4.04	2.95
1	9.2	15.72	2.92	2.61
2	9.2	18.5	4.04	2.95
3	9.2	21.26	5.34	3.25
4	9.2	24.74	7.23	3.57

The measured P_e value for each nozzle appeared to reduce and vary linearly with P_o/P_a in both underexpanded or overexpanded ranges, until a condition was reached where slight deviation from this linear variation appeared before a sudden increase in P_e was recorded. This deviation from the linear variation marked the onset of nozzle separation, as recorded at the tapping location, and the sudden jump in P_e indicated the arrival of the shock wave at the pressure tapping on the inner surface of the nozzle. Figure 1 also shows that the measured static pressure for a given P_o/P_a is always higher than the corresponding theoretical value. This is because the center of the pressure tapping was not exactly at the nozzle exit but at some small distance upstream (2.6 and 1.5 mm for nozzles D and 1, respectively). For this reason, the measured P_e for nozzle 1 appeared to be closer to the theoretical values than that of nozzle D. Theoretical calculations were also performed but with a nozzle diameter corresponding to the center of the pressure tapping for each nozzle. These are also shown in Fig. 1 and appear to be very close to the measured values. From this, on the other hand, it can be said that the experimental and theoretical values of P_e would coincide if the center of the static pressure tapping was located exactly at the nozzle exit. The theoretical line calculated for each nozzle was therefore considered to represent the actual P_e for each nozzle. Ignoring the effect of boundary layer at the inner surface of the nozzle, the actual nozzle separation condition that starts at the nozzle exit was therefore taken to be the intersection points 1_s and D_s between the line joining the recorded separation points at tapping locations on both nozzles 1 and D and the theoretical P_e line at the nozzle exit for each nozzle. These were $P_o/P_a = 16$ and 10.83 for nozzles D and 1, respectively.

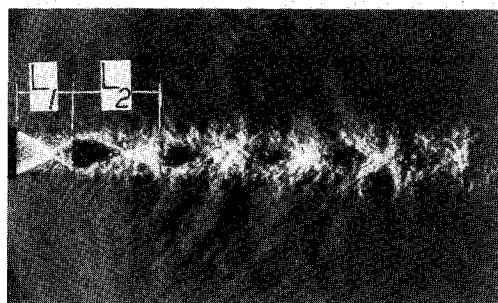
A sample schlieren record obtained with nozzle 1 for three different P_o/P_a is shown in Fig. 2 for both highly underexpanded and overexpanded ranges of jet conditions. The length of any shock cell in the jet plume, as indicated in these pictures, is the distance between the shock extremities in the shear layer for successive cells. The first visible length L_1 was always measured from the nozzle exit plane.

Shock-Cell Length

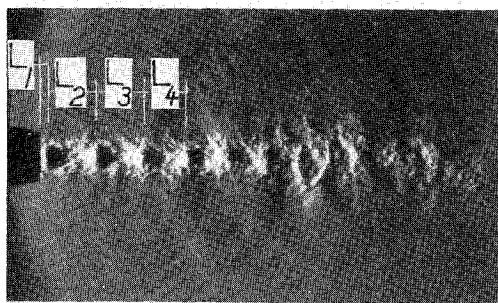
The experimental values for the lengths of the first and second shock cells for nozzle 1 are shown in Fig. 3. The stagnation pressure varied over such a range that the jet at the nozzle exit varied from highly overexpanded to highly under-



a) - $P_o/P_a = 33.31$



b) - $P_o/P_a = 9.84$



c) - $P_o/P_a = 5.08$

Fig. 2 Sample schlieren record obtained with nozzle 1 at different jet operating conditions: a) underexpanded; b) and c) highly overexpanded.

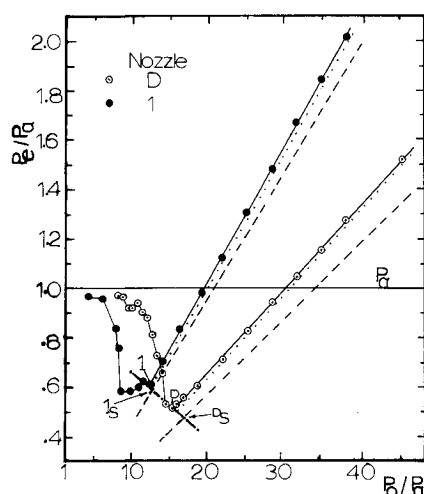


Fig. 1 Variation of static pressure at the nozzle exit with jet stagnation pressure ratio; —, measured at the tapping location; ·····, theoretical at the pressure tapping and nozzle exit planes respectively; 1, 1_s , separation at the tapping location and nozzle exit for nozzle 1 respectively; D, D_s , separation at the tapping location and nozzle exit for nozzle D respectively - - - - , separation line.

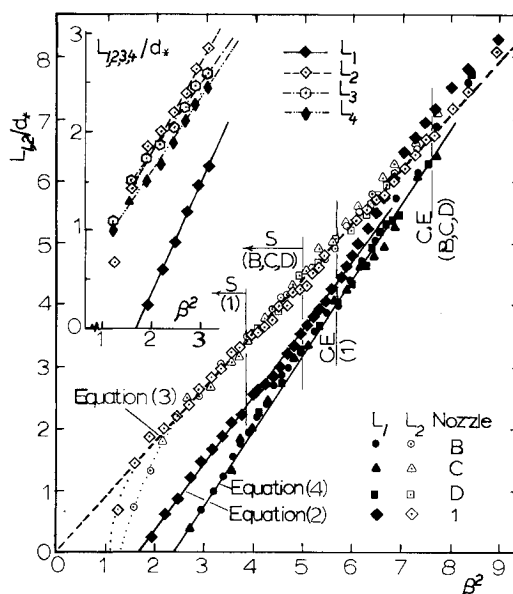


Fig. 3 Variation of shock-cell length with β^2 for nozzles B, C, and D of the first family, and nozzle 1 of the second family; ······ variation of L_2 in the severe nozzle separation range; C.E., correctly expanded.

expanded. Although results for the first two shock cells were available for the whole range, images of the third and fourth cells were sufficiently distinct for reliable measurements only in the highly overexpanded range. The results are presented in Fig. 3 as $L_{1,2}/d_*$ vs β^2 .

The length of the first shock cell L_1 relative to that of the second L_2 as shown in Fig. 2 appears to vary with jet operating conditions. In the highly underexpanded range, $\beta^2 > 6.9$, the length of the first shock cell appeared always to be longer than that of the second or $L_1 > L_2$, and $L_1 = L_2$ at $\beta^2 = 6.9$. In the lower range of β^2 , the opposite is evident or $L_1 < L_2$ in the range $1.7 < \beta^2 < 6.9$. The lower limit $\beta^2 = 1.7$ of this range corresponds to $L_1 = 0$ that marks the disappearance of the first shock cell completely inside the nozzle. The photograph in Fig. 2c is very close to this condition. A point of interest in this range is the jet operating condition $\beta^2 = 6$, where the apparent value for L_1 as defined in Fig. 2 started to vary linearly with β^2 in the range $1.7 < \beta^2 < 6.0$ as

$$L_1/d_* = 1.60\beta^2 - 1.80 \quad (2)$$

The upper limit of this range $\beta^2 = 6$ is the operating condition that is close to $\beta^2 = 5.81$ that corresponds to the nozzle expansion ratio $A_e/A_* = 2.92$, or at which the jet is said to be correctly expanded. Thus the linear dependence of L_1 on β^2 is only exhibited in the overexpanded range of jet-operating conditions. On the other hand, and in the whole range of $\beta^2 > 1.7$, the variation of L_2 with β^2 can be described with the following linear relationship:

$$L_2/d_* = 0.87\beta^2 \quad (3)$$

When β^2 was reduced below the limit $\beta^2 = 1.7$, L_2 continued to decrease but at a faster rate with obvious departure from the above linear dependence on β^2 described by Eq. (3). This is because in this range part of the second shock cell started to disappear inside the nozzle, and it is believed that this linear dependence on β^2 would continue to take place if the nozzle were transparent and the full length of the second shock cell could be measured. In applying the same argument to the first shock cell, the linear dependence of L_1 on β^2 described in Eq. (2) then would not be true for the actual L_1 in the whole range of $1.7 < \beta^2 < 6.0$ but only in the range where no portion of the cell was obscured by the opaque nozzle image in the photographs and where this range could not be determined with reasonable accuracy. In the range $\beta^2 < 1.7$, the third shock cell appeared in the photographs to be completely outside the nozzle, and its measured value appeared to replace L_2 in its linear dependence on β^2 , Eq. (3). From this it is clear that the relative behavior of L_1 and L_2 in the range $1.7 < \beta^2 < 6.0$ is at least qualitatively similar to the relative behavior of L_2 and L_3 in the range $1.1 < \beta^2 < 1.7$. At $\beta^2 = 1.1$ the second shock cell has completely disappeared into the nozzle. Below this highly overexpanded nozzle operating range, accurate detection and evaluation of shock-cell lengths proved to be very difficult, and the matter was not pursued any further. From the L_3 and L_4 values compared with L_1 and L_2 in Fig. 3 in the range $\beta^2 < 3$, it was found on the average that $L_3 = 0.94L_2$ and $L_4 = 0.87L_2$.

Results for nozzles B, C, and D from the first family of fixed expansion ratio $A_e/A_* = 4.04$ are also shown in Fig. 3, mostly in the overexpanded range of jet-operating conditions for both L_1 and L_2 . As is to be expected, L_2/d_* for each of the three nozzles collapsed onto a single characteristic that roughly displayed the same linear dependence on β^2 as was the case with nozzle 1, or $L_2/d_* = 0.87\beta^2$. In the range $2.4 < \beta^2 < 7.4$, the apparent L_1 values for the three nozzles appeared also to collapse onto a single characteristic and to vary linearly with β^2 as

$$L_1/d_* = 1.20\beta^2 - 2.90 \quad (4)$$

which is different from the empirical linear relationship Eq. (2) found with nozzle 1 of different expansion ratio. In this case, $L_1 = 0$ occurred at $\beta^2 = 2.4$. The upper limit $\beta^2 = 7.4$ is close to $\beta^2 = 7.7$, which corresponds to $A_e/A_* = 4.04$, or the condition where the jet is said to be correctly expanded. The lengths of the third and fourth shock cells were measured for nozzle B in the highly overexpanded range of jet stagnation pressures. It was found on the average that $L_3 = 0.94L_2$, and $L_4 = 0.88L_2$.

The nozzle exit flow separation conditions for nozzle 1 and for nozzle D that represents the first family of fixed A_e/A_* obtained from Fig. 1 are also indicated in Fig. 3. In the pressure range below or above that which corresponds to nozzle separation condition, the linear variation of L_1 with β^2 shows a tendency to slightly under- or overpredict the shock-cell length respectively. The same can be said about the linear variation of L_2 but only for nozzle 1 as shown in Fig. 3. Apart from this, the effect of nozzle separation on the shock-cell structures appears to be negligible.

For convergent-divergent nozzles, Tam and Tanna²¹ modified the Prandtl formula for the first shock cell ($L_1/d_e = 1.306\beta$) to the new general form for a hypothetical shock cell $L_j/d_j = 1.306\beta$. Comparison between this equation and the results of their experimental data was not provided, but they claimed to obtain good agreement through their measurements of broadband shock-noise peak frequency. We adopted similar modifications, but to the formula presented by Pack¹⁷ for the first shock cell, to take the form

$$L_j/d_j = 1.22\beta \quad (5)$$

and when d_j is related to the nozzle throat diameter

$$\frac{L_j}{d_*} = 1.22 \frac{1}{(M_j)^1 - 2} \left[\frac{1 + \frac{\gamma - 1}{2} M_j^2}{\frac{\gamma + 1}{2}} \right]^{(\gamma + 1)/4(\gamma - 1)} \cdot \beta \quad (6)$$

Thus for air, Eq. 6 is simplified as:

$$L_j/d_* = 0.928(1 + 0.2M_j^2)^{1.5} [(M_j^2 - 1)/M_j]^{0.5} \quad (7)$$

This equation, which is free from empirical constants, is compared with the measured L_2 values in Fig. 4. Within the limits of experimental error, an excellent agreement is evident over most of the jet operating conditions. In the highly overexpanded jet operating condition, this agreement continued to take place even beyond the conditions where separation of nozzle flow is known to have occurred as is shown in Fig. 4. Some deviation is apparent, but in the severely overexpanded jet conditions $\beta^2 < 3.3$.

Discrete Tone Emission

Shock-associated noise (discrete frequency or broadband) will be emitted from a supersonic jet when the jet is incorrectly expanded. For a supersonic jet issuing from a convergent nozzle this is always the case, since for the jet to be supersonic it is necessarily underexpanded. In the case of a convergent-divergent nozzle, the jet can be supersonic and shock free when it is correctly expanded and when the nozzle is operated at the "design" pressure ratio that corresponds to the nozzle expansion ratio. When the jet is operated at less or more than the design stagnation pressure, the jet is over- or underexpanded respectively. The shock-cell structure is present in both operating ranges, and the shock-associated noise is always emitted in addition to the jet-mixing noise. It is beyond the scope of this paper to present all of the noise data for the nozzles tested, but to emphasize the above facts, the overall sound-pressure level and the discrete tone amplitude as functions of P_o/P_a for nozzle B are shown in Fig. 5. The corresponding discrete tone frequencies for the same nozzle

are also presented. In the range $29 < P_o/P_a < 32$, no discrete tones were detected, and the overall sound-pressure level emitted by the jet was at a minimum and presumably consisted solely of turbulent jet-mixing noise as is shown in Fig. 5c. At this condition the jet was nearly correctly expanded so that the shocks in the jet could be expected to be of minimum strength. On a one-dimensional inviscid basis, the nozzle was theoretically correctly expanded at $P_o/P_a = 34$; in fact, the nozzle was conical so that the flow was not one-dimensional, and for this reason the jet was not quite shock free. This was evident in the schlieren photographs. On both sides of this P_o/P_a range, the overall sound-pressure level increased in value due to the strengthening of the shock-cell structure. A maximum was reached in the low-stagnation pressure range at $P_o/P_a \approx 10$ and then dropped rapidly as P_o/P_a was decreased further. The discrete tone amplitude is shown in Fig. 5b, which roughly displays a behavior similar to that at the overall sound-pressure level. Again, on both sides of the $P_o/P_a \approx 29$ – 32 range, the discrete tone amplitude increases as the jet is more incorrectly expanded. In the overexpanded range, the maximum amplitude appears to occur at $P_o/P_a \approx 12$; in this region, the measured amplitude variation suggested instability in the mechanism responsible for the shock-generated noise. It is worth mentioning that the Mach reflection configuration started to replace the regular reflection at the jet centerline at $P_o/P_a \approx 13.5$, and this might have caused this instability. Typical examples of the noise spectra emitted by this nozzle in the overexpanded, nearly correctly expanded, and underexpanded pressure ranges are shown in Figs. 6a, 6b, and 6c respectively. The discrete tone frequency shown in Fig. 5a is a decreasing function with increasing P_o/P_a . Apart from two slight discontinuities as indicated in Figure 5a, the function is considered to be more or less continuous. The first discontinuity occurred at $P_o/P_a \approx 21$ in the overexpanded range of P_o/P_a and cannot be related to a particular jet operating condition. The second occurred around the region where the jet displayed the characteristics of being correctly expanded and where the discrete tone could not be detected. The harmonics for the fundamental discrete tone frequency were rarely present in the noise spectra measured, although some other tones of minor amplitudes were sometimes detected. The amplitude of the harmonics is usually much less than that of the fundamental, and it appeared from the noise spectra that they were masked by the broadband component that hindered their detection.

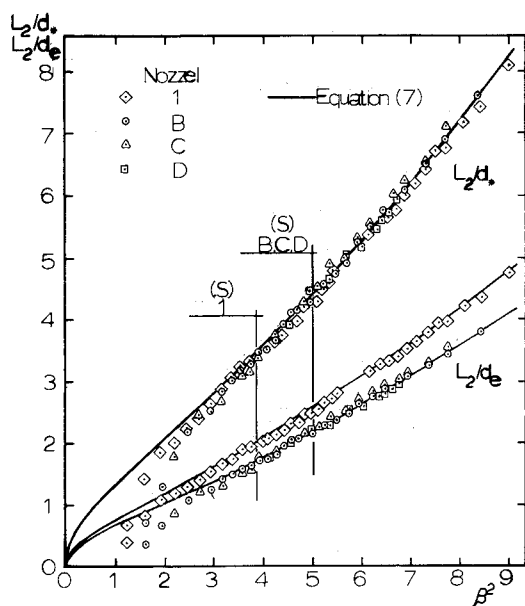


Fig. 4 Comparison between experimental values for the second shock-cell length and Pack's modified formula; Eq. (7).

The measured discrete tone frequencies for nozzles of the first family are presented as functions of jet stagnation pressure P_o/P_a in Fig. 7. Apart from slight discontinuities that appeared in the vicinity of $P_o/P_a \approx 21$ and $P_o/P_a \approx 31$, and at some other values of stagnation pressure that varied for different nozzles but appeared unrelated, these frequency characteristics are considered to be continuous. The wavelengths of the discrete tones normalized with the corresponding nozzle throat and exit diameters as a function of β^2 are presented in Fig. 8. It is clear that λ/d^* for the five nozzles collapsed together to define a single characteristic. All nozzles in this family have the same expansion ratio $A_e/A_* = 4.04$; therefore λ/de is also a single characteristic as shown in Fig. 6. The discrete tone frequencies measured for the second family of nozzles of the same throat diameter $d^* = 9.2$ mm but with different A_e/A^* are shown in Fig. 9. In this case the discrete tone frequencies measured for all of the four nozzles collapsed onto a single characteristic. Naturally, the λ/d^* values as a function of β^2 define a single characteristic that is shown in Fig. 10, and is the same as the λ/d^* characteristic of the first

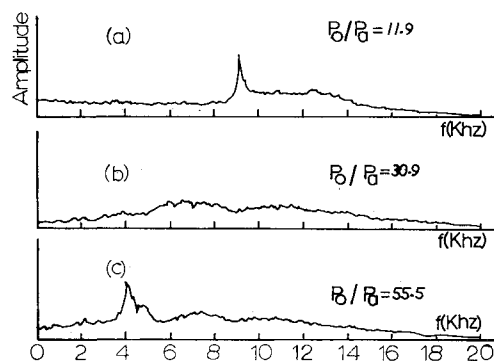


Fig. 5 The frequency and amplitude of the fundamental discrete tone, and the overall sound-pressure level obtained with nozzle B of the first family; A is the pressure range where discrete tones could not be detected.

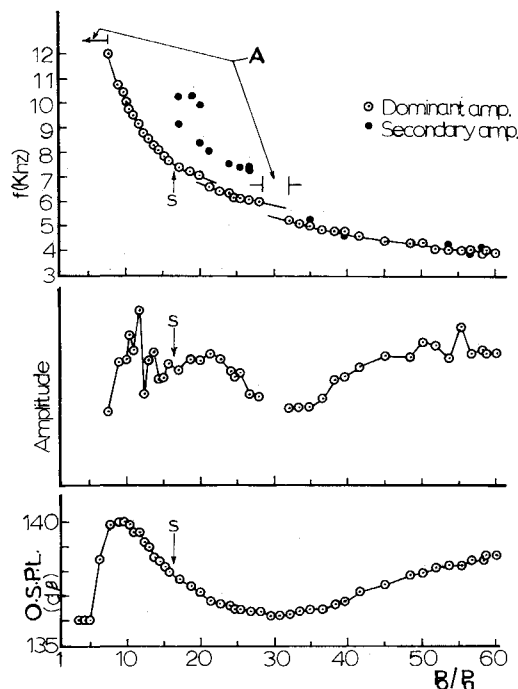


Fig. 6 Noise spectra obtained with nozzle B for different jet operating conditions; a) overexpanded, $P_o/P_a = 11.9$; b) nearly correctly expanded, $P_o/P_a = 30.9$; c) underexpanded, $P_o/P_a = 55.5$.

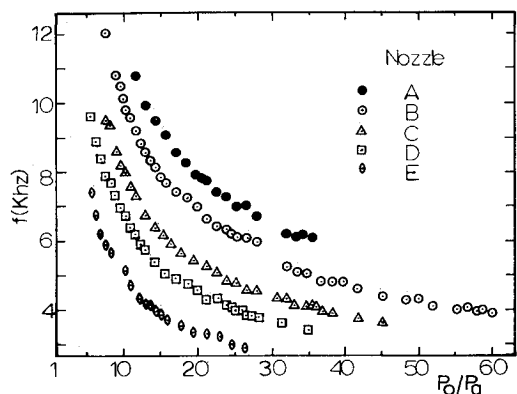


Fig. 7 Discrete tone fundamental frequency as a function of jet stagnation pressure ratio obtained with nozzles of the first family.

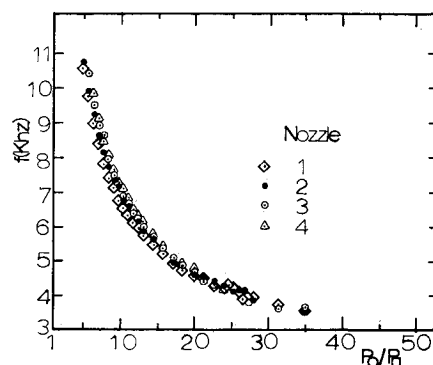


Fig. 9 Discrete tone fundamental frequency as a function of jet stagnation pressure ratio obtained with nozzles of the second family.

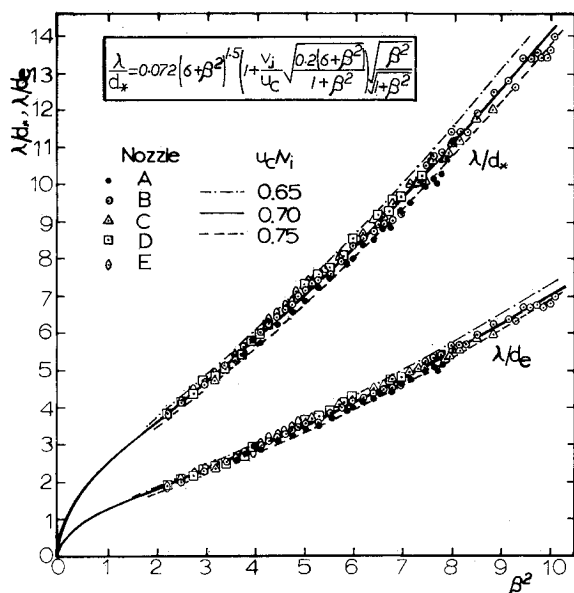


Fig. 8 The measured nondimensional wavelength of the discrete tone fundamental frequency as a function of β^2 obtained with nozzles of the first family; —, —·—, —·—·—; theory: Eq. (1) with Eq. (7); $\bar{L} = 0.87L_j$.

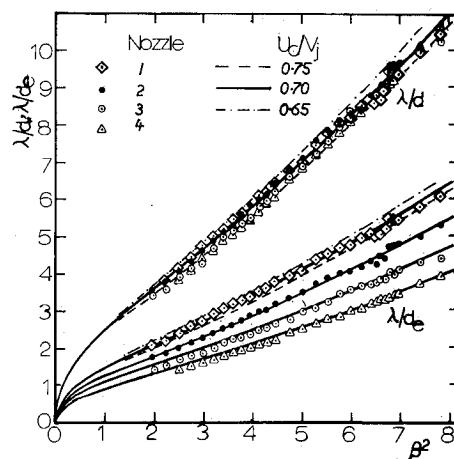


Fig. 10 The measured nondimensional wavelength of the discrete tone fundamental frequency as a function of β^2 , obtained with nozzles of the second family —, —·—, —·—·—; theory: Eq. (1) with Eq. (7); $\bar{L} = 0.87L_j$.

family. The results for the second family were only separated for different nozzles when presented as λ/de vs β^2 that are also shown in Fig. 10.

Comparison with Theory

The experimental data for the discrete tone wavelength obtained for all nozzles tested and normalized with nozzle throat and exit diameter are compared in Figs. 8 and 10 with theoretical curves obtained from Powell's simplified Eq. (1) for the feedback mechanism ($\lambda/L = 1 + c_o/u_c$). The length scale L in this equation is the length of the shock cell in the vicinity of screech source. This is usually represented by an average cell length \bar{L} , which was found in the previous section to be $\bar{L} \approx 0.87L_2$, which roughly represents the fourth shock-cell length and is very close to that of Harper-Bourne and Fisher.²⁰ From the agreement shown in Fig. 4 between the measured L_2 values and the theoretical L_j from Eq. (7), \bar{L} was taken as $\bar{L} = 0.87L_j$. Substituting $0.87L_j$ for L in Eq. (1)

$$\lambda/(0.87L_j) = 1 + c_o/u_c \quad \text{or} \quad \lambda/d_* = 0.87L_j/d_*(1 + c_o/u_c)$$

and in its final form in terms of u_c/V_j and β^2 is included in Fig. 8. The disturbance convection velocity used was the generally accepted value of $u_c/V_j = 0.70 \pm 0.05$ (see Refs. 8, 15, 20, 23, and 26–30). The theoretical curves are shown in

each figure for three different values of u_c/V_j ; namely, 0.65, 0.70, and 0.75. The agreement between theory and experiments that is evident in Figs. 8 and 10 is excellent for all nozzles tested. Apart from the apparent tendency of the measured λ/d_* to agree better with the higher values of u_c/V_j range (0.70–0.75), especially in the high range of jet pressure, most of the experimental data appear to be confined between the two theoretical curves corresponding to $u_c/V_j = 0.65$ and 0.75, with $u_c/V_j = 70\%$ as a good representative. This agreement indicates that the proposed theoretical prediction for the shock-cell length combined with Powell's equation closely represents the actual process of discrete tone generation, even in the jet pressure range where separation of the nozzles is known to have occurred.

The experimental points for λ/\bar{L} measured for nozzles B, C, D, and 1 are also compared with theoretical curves obtained from Powell's Eq. (1) as λ/\bar{L} vs β^2 in Fig. 11. Also included in Fig. 11 is Powell's equation in terms of u_c/V_j and β^2 . The average cell length \bar{L} was taken as $\bar{L} = 0.87L_2$, where L_2 in this case was the actually measured value shown in Fig. 4. Some scatter of the data in this figure is obvious, and this is due to both λ and L_2 were actually the measured experimental values for a given P_0/P_a . This scatter is highlighted by the fact that the scale of the ordinate λ/\bar{L} in Fig. 11 is larger than those λ/d_* in Figs. 8 and 10 by a factor of more than 13. Figure 11 shows that in the range $\beta^2 < 3$ all the experimental points appear to be relatively high. This is understandable, since in this range the nozzle flow was severely separated, and the measured L_2 values were always lower than the corresponding theoretical L_j values obtained from Eq. 7, as is

shown in Fig. 4. Nevertheless, in the range $\beta^2 > 3$, it is obvious that most of the experimental points are confined between the two theoretical curves corresponding to u_c being 65–75% of the fully expanded jet velocity but with the apparent trend that the experimental results tend to follow a curve that is steeper than that of Powell's equation. This trend mismatch is examined through the assumptions made to arrive at the results in Fig. 11. The first assumption of $\bar{L}/L_2 = 0.87 = \text{const}$ might not be true in the whole range of β^2 , and the trend mismatch could be removed if \bar{L}/L_2 varied with β^2 . This could not be verified in the current experiments since it was not noticed in the relatively low β^2 range, and it was difficult to perform measurements of shock-cell lengths at shock locations far downstream of the nozzle exit with reasonable accuracy in the high range of β^2 . Empirical formulas for \bar{L} as an increasing function of β are found in Refs. 18 and 27, but these are different for different nozzles. With regard to the assumed relationship between u_c and V_j , roughly in the range $3 < \beta^2 < 5.4$ the experimental results agree with the range $u_c/V_j = 0.65$ –0.70, and in the range $\beta^2 > 6.0$ agree with $u_c/V_j = 0.68$ –0.77. This means that u_c/V_j is not constant and should increase with β^2 . In fact, the experimental λ/d_* values in Figs. 8 and 10 appear to favor higher values of u_c/V_j in the high range of β^2 . Higher values for u_c/V_j , 0.7–0.80 and 0.815, were reported in Refs. 25 and 16, respectively. In the above, Powell's simplified equation was assumed to be correct, but this is not perfectly true since the actual frequency of the fundamental discrete tone is a more complicated function of the various lengths involved.^{4,5} However, from the general agreement displayed in Figs. 8, 10, and 11, the simplified equation appears to provide a good approximation to represent the process of discrete tone generation.

Comparison with Previous Investigations

The empirical relationships which were presented by Mamin et al.¹⁶ for L_1 , L_2 and compared with the corresponding present experimental values obtained with nozzle 1 in Fig. 12. Poor agreement can be noticed between their empirical relationship for L_1 and the current measurements, especially in the overexpanded range $3.88 < \beta^2 < 5.8$ and $\beta^2 > 6.65$ in the over- and underexpanded ranges of the jet, respectively. This disagreement might be due to the fact that their nozzles were designed for parallel flow at the nozzle exit, and the departure of the apparent L_1 from its true value in the overexpanded range was magnified by the conical type of the nozzles used in the current investigation. For the L_2 , the only apparent agreement is in the overexpanded range $3.88 < \beta^2 < 5.8$ or between separation and the correctly expanded condition of nozzle 1, but gross disagreement is obvious, especially in the high range of β^2 . In the high range of β^2 , they imposed the condition that $L_1 = L_2$ in the range $P_e/P_a > 1.5$. This is contrary to the current results where $L_1 = L_2$ occurred only at $\beta^2 \approx 6.88$ that corresponds to $P_e/P_a = 1.36$ and $L_1 > L_2$ in the range $\beta^2 > 6.88$. By contrast, their empirical relationship for the fundamental discrete tone wavelength, although it predicts slightly lower values than those of the theoretical curve at higher values of β^2 , is in general considered to be in fair agreement in most of the range covered by the current investigation. In the low-pressure range, on the other hand, its agreement with the measurements of other investigators is rather excellent.

The current L_1 values are also compared in Fig. 12 with the semiempirical relations presented by Love et al.¹⁹ for L_1 as measured from the nozzle exit plane of high-pressure ratio conical nozzles. In the underexpanded range $3.88 < \beta^2 < 5.8$, the current L_1 values appear to be slightly higher than those predicted by their formula. This deviation appears to increase with β^2 in the underexpanded range of the jet or where the present L_1 values deviates from the linear dependence on β^2 [see Eq. (2)]. This deviation in the high-pressure range was also mentioned in their report, but at higher P_e values than those with nozzles in the current investigation.

The experimental results of Seiner and Norum²⁰ for L_2 obtained with a Mach 2 nozzle designed for parallel flow at the exit are also compared with the current results in Fig. 12. Their four experimental points for L_2 replotted from their paper appear to agree very well with the current experimental data. However, their empirical relationship for L_2 developed for their Mach 2 nozzle deviates sharply from the current experimental results when extrapolated to higher jet stagnation pressure ratios, $\beta^2 > 5.2$. Also shown in Fig. 12 are the discrete tone frequency measurements reported by Seiner and Norum,²⁰ Yu and Seiner,¹⁴ and Powell.⁵ All of these data points joined those at the current investigation in defining a single characteristic that can be predicted fairly well by Powell's loop equation in most of the jet pressure range. In the low-pressure range where discrete tone could not be detected with the current conical nozzles, some deviation from Powell's equation starts to take place. This suggests that some variation

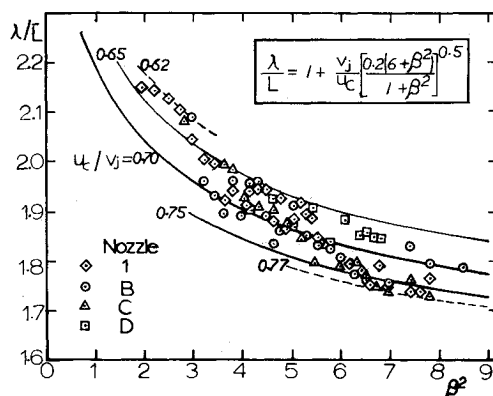


Fig. 11 Comparison between the measured λ/\bar{L} with those predicted by Powell's feedback mechanism, Eq. (1); $\bar{L} = 0.87$ ($L_1 = L_2$).

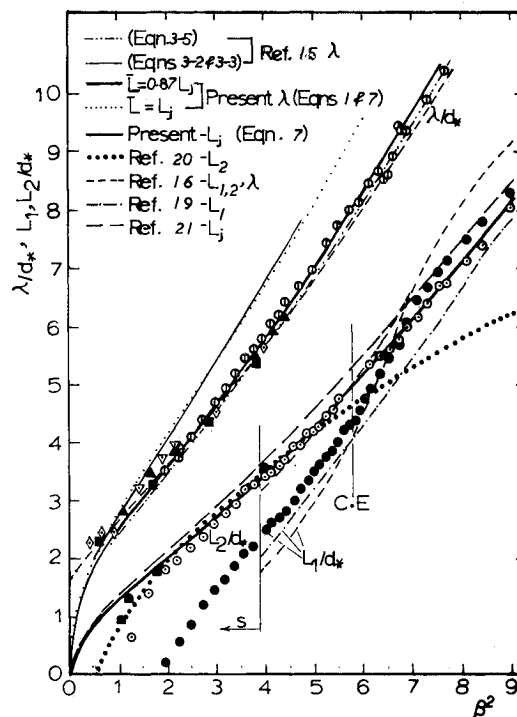


Fig. 12 Comparison between the experimental results obtained with nozzle 1 and those of previous investigations; $\bullet, \circ, \triangle, \square$, L_1/d_* , L_2/d_* , and λ/d_* , respectively, measured with nozzle 1; \bullet , L_2/d_* , for $M = 2$ nozzle from Ref. 20; $\diamond, \triangle, \square$, λ/d_* , for $M = 1$, $M = 1.5$, and $M = 2$ nozzles from Ref. 20; ∇ , λ/d_* , for $M = 2$, from Ref. 14.

in the mechanism responsible for their generation must have occurred.

The L_j equation used by Tam and Tanna²¹ in the vortex sheet theory that was developed for nozzles designed for parallel flow at the exit is also compared with the present shock-cell lengths in Fig. 12. In essence, this equation is the same as that of the current Eq. (7) but with a different factor 0.994 instead of 0.928, and this is due to their use of Prandtl's $k = 1.306$ rather than Pack's $k = 1.22$. As is expected, their equation overpredicted the L_2 measurements in all the β^2 range, but agreed rather well with L_1 in the high underexpanded range before L_1 started to shrink with reducing pressure at $\beta^2 = 7$. For screech frequency prediction, Tam et al.¹⁵ developed a semiempirical relation in terms of $f D_j / V_j$, [Eqs. (3–5) in their paper], which can also accommodate jets with elevated stagnation temperatures. This relation was derived by incorporating L_j in a theoretical equation they derived for the broadband shock-noise peak frequency but at the special case of the angle of noise radiation from the jet axis being 180 deg. The form of their theoretical relation at this limit is in fact the same as that of Powell's Eq. (1) for the feedback mechanism. Therefore, their semiempirical relation for unheated jets in terms of λ/d_* is exactly the same as that derived in this paper and included in Fig. 8 but with a slightly different factor of 0.0711 instead of 0.0722. This difference is due to their assumption of \bar{L} being $0.80L_j$ together with Prandtl's $k = 1.306$, rather than $\bar{L} = 0.87L_j$ and Pack's $k = 1.22$, respectively. Their relation is also shown in Fig. 12 and appears to be in good agreement with those of the present investigation. The solution for their theoretical Eqs. (3–2) and (3.3) replotted from their paper (see Fig. 6) is also compared in Fig. 12 with the λ/d_* curve obtained for $u_c/v_j = 0.70$ and $\bar{L} = L_j$ from the current Eq. (7) with Eq. (1). It is interesting to note that there is hardly any difference between the two curves, and this suggests that the assumed $u_c/v_j = 0.70$, which is the only empirical factor used to obtain our curve must have been equal or very close to its theoretical value.

Conclusions

The main conclusions derived from this investigation are as follows:

- 1) In the whole of the highly underexpanded and most of the overexpanded ranges of jet operating conditions, it was found that the second shock-cell length could be predicted using a modification of Pack's theoretical formula for the first shock-cell length of a slightly incorrectly expanded supersonic jet. Pack's formula was modified by replacing the nozzle diameter with the jet diameter corresponding to the fully expanded jet Mach number. Deviation between theory and experiment was only noticed in the highly overexpanded range, $\beta^2 < 3.3$, or in the range of severe nozzle flow separation.
- 2) To a good approximation, the length of the second shock cell appeared to display a linear dependence on β^2 in most of the pressure range of the current investigation, rather than on β as predicted by Prandtl and Pack for slightly incorrectly expanded jets, and experimentally verified by others in a relatively low range of jet pressure ratios. This apparent linear variation with β^2 was evident in a wide range of over- or underexpanded jet operating conditions, especially in the overexpanded range, and was found to be the same for all nozzles tested.
- 3) As is to be expected, the first shock cell appeared to be longer than the second in most of the underexpanded range of jet operating conditions. In the whole of the overexpanded range, its apparent length as measured from the nozzle exit plane appeared to be shorter than the second and to vary linearly with β^2 . The proportionality constant in this linear variation was found to vary with nozzle expansion ratio.
- 4) Discrete tone frequencies, as measured from the far field with a fixed microphone, could not be detected in the

very low range of jet stagnation pressures and in the range corresponding to the correct expansion of the nozzles.

5) The wavelength of the fundamental discrete tone and the length of the second shock cell were found not to depend on the nozzle exit diameter but were inversely proportional to the nozzle throat diameter. On the other hand, the apparent length of the first shock cell was found to be different for different nozzle expansion ratios.

6) With a constant ratio between the convection velocity and the fully expanded jet velocity and the use of Pack's modified theoretical formula for the first shock-cell length in Powell's simplified loop equation, the wavelength of the fundamental discrete tone could be predicted to a good practical accuracy. This indicates that Powell's equation is an excellent representation of the actual discrete tone generation process.

7) Discrete tones continued to be emitted and to be predictable by Powell's equation in the jet pressure range of severe nozzle flow separation.

References

- ¹Abdel-Fattah, A.M., "Duct Resonance in High Pressure Ratio Thrust Augmenting Ejectors," *Proceedings of the 2nd Workshop on Wind Engineering and Industrial Aerodynamics*, Commonwealth Scientific and Industrial Research Organization, Melbourne, Australia, Aug. 1985.
- ²Abdel-Fattah, A.M. and Favaloro, S.C., "Duct Resonance and Its Effect on the Performance of High Pressure Ratio Thrust Augmenting Ejectors," *Proceedings of the 8th International Symposium on Air Breathing Engines*, June 1987, pp. 531–539.
- ³Fisher, S.A. and Irvine, R.D., "Air Augmentation of Rockets for Low Speed Application," 5th International Symposium on Airbreathing Engines, Feb. 1981, Bangalore, India.
- ⁴Powell, A., "On the Noise Emanating From a Two-dimensional Jet Above the Critical Pressure," *The Aeronautical Quarterly*, Vol. 4, Feb. 1953, pp. 103–122.
- ⁵Powell, A., "On the Mechanism of Choked Jet Noise," *Proceedings of the Physical Society*, Vol. B66, London, Dec. 1953, pp. 1039–1056.
- ⁶Davies, M.G. and Oldfield, D.E.S., "Tones from a Choked Axisymmetric Jet. I. Cell Structure, Eddy Velocity and Source Locations and II. The Self Excited Loop and Mode of Oscillation," *Acoustica*, Vol. 23, April 1962, pp. 257–277.
- ⁷Hammit, A.G., "The Oscillation and Noise of an Overpressure Sonic Jet," *Journal of the Aerospace Sciences*, Vol. 28, Sept. 1961, pp. 673–680.
- ⁸Glass, D.R., "Effect of Acoustic Feedback on the Spread and Decay of Supersonic Jets," *AIAA Journal*, Vol. 6, Oct. 1968, pp. 1890–1897.
- ⁹Jungowski, W.M., "Influence of Closely Located Solid Surfaces on the Sound Spectra Radiated by Gas Jet," *Proceedings of International Union of Theoretical and Applied Mechanics/International Commission on Acoustics/AIAA Symposium*, Aug. 1979, pp. 116–122.
- ¹⁰Nagel, R.T., Denham, J.W., and Papathanasiou, A.G., "Supersonic Jet Screech Tone Cancellation," *AIAA Journal*, Vol. 21, Nov. 1983, pp. 1541–1545.
- ¹¹Norum, T.D., "Screech Suppression in Supersonic Jets," *AIAA Journal*, Vol. 21, Feb. 1983, pp. 235–240.
- ¹²Lassiter, L.W. and Hubbard, H.H., "The Near Noise Field of Static Jets and Some Model Studies of Devices for Noise Reduction," NACA TN-3187, July 1954.
- ¹³Sharman, P.M., Glass, D.R., and Duleep, K.G., "The Jet Flow Field During Screech," *Applied Scientific Research*, Vol. 32, Aug. 1976, pp. 283–303.
- ¹⁴Yu, J.C. and Seiner, J.M., "Nearfield Observations of Tones Generated from Supersonic Jet Flows," AIAA Paper 83-0706, 1983.
- ¹⁵Tam, C.K.W., Seiner, J.M., and Yu, J.C., "Proposed Relationship Between Broadband Shock Associated Noise and Screech Tones," *Journal of Sound and Vibration*, Vol. 110, Oct. 1986, pp. 309–321.
- ¹⁶Mamin, V., Pykhov, Z., and Rimski-Korsakov, A., "Discrete Tone Radiation Arising from a Supersonic Jet Flowing into an Unlimited Gaseous Medium and into a Cylindrical Ejector," *Proceedings of the 7th International Congress on Acoustics*, paper no. 24N11, 1971, pp. 469–472.
- ¹⁷Pack, D.C., "A Note on Prandtl Formula for the Wave Length of a Supersonic Gas Jet," *Quarterly Journal of Mechanics and Applied Mathematics*, Vol. 3, Pt. 2, 1950, pp. 173–181.

¹⁸Harper-Bourne, M. and Fisher, M.J., "The Noise from Shock Waves in Supersonic Jets," AGARD CP-131, Sept. 1973, pp. 11-1-11-13.

¹⁹Love, E.S., Grigsby, C.E., Lee, L.P., and Woodling, M.J., "Experimental and Theoretical Studies of Axisymmetric Free Jets," NASA TR-6, 1959.

²⁰Seiner, J.M. and Norum, T.D., "Experiments of Shock Associated Noise on Supersonic Jets," AIAA Paper 79-1526, July 1979.

²¹Tam, C.K.W. and Tanna, H.K., "Shock Associated Noise of Supersonic Jets from Convergent-Divergent Nozzles," *Journal of Sound and Vibration*, Vol. 81, April 1982, pp. 337-358.

²²Tam, C.K.W., Jackson, J.A., and Seiner, J.M., "A Multiple-Scales Model of the Shock Cell-Structure of Imperfectly Expanded Supersonic Jets," *Journal of Fluid Mechanics*, Vol. 153, April 1985, pp. 123-149.

²³Tanna, H.K., "An Experimental Study of Jet Noise; Part II: Shock Associated Noise," *Journal of Sound and Vibration*, Vol. 50, 1977, pp. 429-444.

²⁴Pao, S.P. and Seiner, J.M., "Shock Associated Noise in Supersonic Jets," *AIAA Journal*, Vol. 21, May 1983, pp. 687-693.

²⁵Lowson, M.V. and Ollerhead, J.B., "Visualization of Noise from Cold Supersonic Jets," *Journal of the Acoustical Society of America*, Vol. 44, Nov. 1968, pp. 624-630.

²⁶Seiner, J.M. and Yu, J.M., "Acoustic Near Field Properties Associated with Broadband Shock Noise," *AIAA Journal*, Vol. 22, Sept. 1984, pp. 1207-1215.

²⁷Norum, T.D. and Seiner, J.M., "Broadband Shock Noise from Supersonic Jets," *AIAA Journal*, Vol. 20, Jan. 1982, pp. 68-73.

From the AIAA Progress in Astronautics and Aeronautics Series...

ORBIT-RAISING AND MANEUVERING PROPULSION: RESEARCH STATUS AND NEEDS—v. 89

Edited by Leonard H. Caveny, Air Force Office of Scientific Research

Advanced primary propulsion for orbit transfer periodically receives attention, but invariably the propulsion systems chosen have been adaptations or extensions of conventional liquid- and solid-rocket technology. The dominant consideration in previous years was that the missions could be performed using conventional chemical propulsion. Consequently, major initiatives to provide technology and to overcome specific barriers were not pursued. The advent of reusable launch vehicle capability for low Earth orbit now creates new opportunities for advanced propulsion for interorbit transfer. For example, 75% of the mass delivered to low Earth orbit may be the chemical propulsion system required to raise the other 25% (i.e., the active payload) to geosynchronous Earth orbit; nonconventional propulsion offers the promise of reversing this ratio of propulsion to payload masses.

The scope of the chapters and the focus of the papers presented in this volume were developed in two workshops held in Orlando, Fla., during January 1982. In putting together the individual papers and chapters, one of the first obligations was to establish which concepts are of interest for the 1995-2000 time frame. This naturally leads to analyses of systems and devices. This open and effective advocacy is part of the recently revitalized national forum to clarify the issues and approaches which relate to major advances in space propulsion.

Published in 1984, 569 pp., 6 × 9, illus., \$49.95 Mem., \$69.95 List

TO ORDER WRITE: Publications Dept., AIAA, 370 L'Enfant Promenade S.W., Washington, D.C. 20024-2518